NIH Public Access
Author Manuscript
ACS Nano. Author manuscript; available in PMC 2009 December 23.

Published in final edited form as:
ACS Nano. 2008 December 23; 2(12): 2481–2488. doi:10.1021/nn800466c.

Detoxification of Gold Nanorods By Treatment With Polystyrenesulfonate

Alexei P. Leonov[†], **Jiwen Zheng**[§], **Jeffrey D. Clogston,**[§], **Stephan T. Stern**[§], **Anil K. Patri**[§], and **Alexander Wei**[†,*]

†*Department of Chemistry, Purdue University, West Lafayette, Indiana 47907*

§*Nanotechnology Characterization Laboratory, Advanced Technology Program, SAIC-Frederick, Inc., NCI-Frederick, Frederick, Maryland, 21702*

Abstract

We address an outstanding issue associated with the biocompatibility of gold nanorods (GNRs), a promising agent for biomedical imaging and theragnostics. GNRs are typically prepared in the presence of cetyltrimethylammonium bromide (CTAB), a cationic surfactant whose rigorous removal is necessary due to its cytotoxicity and membrane-compromising properties. CTAB-stabilized GNRs can be partially purified by treatment with polystyrenesulfonate (PSS), an anionic polyelectrolyte often used as a surrogate peptizing agent, followed by chloroform extraction and ultrafiltration with minimal loss of dispersion stability. However, in *vitro* cytotoxicity assays of PSS-coated GNRs revealed IC_{50} values in the low to submicromolar range, with subsequent studies indicating the source of toxicity to be associated with a persistent PSS—CTAB complex. Further exchange of CTAB-laden PSS with fresh polyelectrolyte greatly improves biocompatibility, to the extent that 85 μg/mL of "CTAB-free" GNRs (the highest level evaluated) has comparable toxicity to a standard phosphate buffer solution. Ironically, PSS is not effective by itself at stabilizing GNRs in CTAB-depleted suspensions: while useful as a detergent for GNR detoxification, it should be replaced by more robust coatings for long-term stability under physiological conditions.

Keywords

Nanorods; nanomedicine; nanobiotechnology; toxicity; dispersion stability

Plasmon-resonant gold nanorods (GNRs) have attracted much recent attention for their potential as multifunctional agents in theragnostics, an integrated approach to diagnostic imaging and therapy.[1,2,3] GNRs are well known for their very high extinction coefficients at near-infrared (NIR) wavelengths; when excited at plasmon resonance, they can serve simultaneously as optical contrast agents and as photothermal transducers capable of mediating local heating effects.[4,5,6,7,8,9] These resonances are tunable as a function of size and shape: the absorption and scattering cross sections both increase rapidly with particle volume, whereas the plasmon frequencies are sensitive to particle anisotropy and aspect ratio. For *in vivo* applications, nanoparticles with NIR resonances are particularly favored because of the relatively high transmittivity of biological tissues in the spectral range between 750 and 1300 nm. Other examples of NIR-absorbing Au nanoparticles used in theragnostic applications include nanoshells,[10,11] nanocages,[12] and aggregates of spherical nanoparticles.[13,14]

*Corresponding author. E-mail: alexwei@purdue.edu

NIH-PA Author Manuscript
NIH-PA Author Manuscript
NIH-PA Author Manuscript

NIH-PA Author Manuscript

NIH-PA Author Manuscript

NIH-PA Author Manuscript

In order to be considered for translation to clinical studies, nanoparticles and their functionalized derivatives must pass a preclinical evaluation commonly referred to as adsorption, distribution, metabolism, excretion and toxicity (ADMET) profiling. These are performed *in vivo* using standard animal models, but are usually preceded by *in vitro* cell-based assays for preliminary evaluation of selective targeting and cytotoxicity. Cell-based assays provide a rapid and cost-effective method for evaluating three practical issues that affect the viability of nanoparticle agents for *in vivo* use: (i) surface functionalization to enable targeted delivery while avoiding nonspecific adsorption and uptake, (ii) long-term dispersion stability in fluids of high ionic strength, as it relates to targeting efficacy, and (iii) minimal cytotoxicity at high dosages. While each issue can be addressed independently in relatively straightforward fashion, addressing all three criteria at once is more challenging because biocompatibility may be compromised by the coatings and surfactants responsible for nanoparticle targeting and dispersion stability, and vice versa.

The criteria above present a particularly vexing problem for anisotropic nanoparticles such as GNRs, whose synthesis involves high concentrations of cetyltrimethylammonium bromide (CTAB), a cationic surfactant with membrane-compromising properties. CTAB has a poor biocompatibility profile, with *in vitro* toxicological studies yielding IC_{50} values in the low micromolar range.[15,16,17] Furthermore, CTAB-coated nanoparticles are susceptible to nonspecific cell uptake, even at very low surfactant levels.[18,19] While submicromolar CTAB concentrations may have little adverse effect on cell viability, the effort to target nanoparticles to diseased cells is nonetheless compromised by residual CTAB, as it heightens the possibility of collateral photothermal damage caused by subsequent NIR irradiation. These studies indicate that GNRs and other formulations containing CTAB will require a rigorous purification procedure prior to clinical testing.[4]

The unresolved issue of biocompatibility belies the numerous methods of surface coating methodologies developed for GNRs and other nanoparticles in recent years.[5-13,19-24] Most of these appear to be useful for exploratory investigations in a laboratory setting, although few if any have been subject to the rigors of thorough preclinical evaluation. For example, a widely used method of nanoparticle coating involves the electrostatic physisorption of polyelectrolytes, which can provide dispersion stability as well as a foundation for immobilizing antibodies or protein biomarkers.[5,8,20,21,22,23,24] However, the stability and biocompatibility of nanoparticles functionalized in this manner cannot be assumed, as the surface binding energies are often variable or attenuated under physiological conditions, with possible leaching of the physisorbed species.

In this paper we evaluate polystyrenesulfonate sodium salt (PSS, 70 kDa) as a peptizing agent and detergent for the efficient removal of CTAB from GNR suspensions. Our interests are driven by a need to identify a reliable and ultimately scalable process for producing batch quantities of GNRs with good dispersion control and low cytotoxicity, to support their application as imaging and theragnostic agents in a clinical setting. PSS is commonly used as a nontoxic peptizing agent in numerous commercial products, and thus generally regarded as a safe additive.[25] However, we find that PSS-coated GNRs can retain surprisingly high levels of *in vitro* cytotoxicity even after exhaustive membrane dialysis or ultrafiltration. We ascribe this to the presence of a persistent PSS—CTAB complex that gradually desorbs from the GNR surface. CTAB also appears to play a cooperative role in PSS adsorption, but the PSS—CTAB complex can be removed from GNRs by centrifugation and replaced with fresh polyelectrolyte or other surfactants, to the point that cytotoxic effects are no longer observed.

NIH-PA Author Manuscript

NIH-PA Author Manuscript

NIH-PA Author Manuscript

Results and Discussion

Peptization of gold nanorods

In previous studies, GNRs were successfully stabilized by treatment with a mixed-bed ion-exchange resin (Amberlite MB-3, Sigma), prior to removal of CTAB by membrane dialysis.[4,19] However, the scalability of this protocol is limited, and its reliability can depend on the source of ion-exchange resin. In particular, we noted that GNRs exposed to older resin beads retained better dispersion stability after removal of CTAB than those treated with newly purchased beads, regardless of mesh size and method of activation. Ion-exchange resins are well known to degrade and release small amounts of polyelectrolytes over time, suggesting that polymer adsorption may be contributing to dispersion stability. Several other studies have shown that GNRs can be coated by PSS and other anionic polyelectrolytes, then functionalized without apparent loss of dispersion stability.[21-24] We thus evaluated a scalable protocol for surfactant exchange based on polyelectrolyte-coated GNRs.

GNRs were synthesized by seeded growth methods in micellar CTAB solutions, then treated with Na_2S and precipitated by centrifugation to separate them from excess CTAB (see Methods for details).[26,27,28] The precipitate was resuspended as a highly concentrated dispersion with an optical density (O.D.) of 16.8, and washed multiple times with chloroform to extract additional CTAB from the GNR suspension. Three washes is sufficient for reducing the CTAB concentration below its critical micelle concentration (CMC; *ca*. 1 mM),[29] but can lead rapidly to GNR flocculation if performed in the absence of a surrogate stabilizing agent. Introduction of 70-kDa PSS after the first wash[30] can provide effective dispersion stability and nearly complete retention of optical density and absorption peak linewidth, even after several rounds of chloroform extraction and membrane ultrafiltration. This conditioning also produces a shift in zeta potential from +29 mV to −51 mV, indicating that PSS replaced CTAB as the dominant adsorbate on the GNR surfaces. After 3 cycles of ultrafiltration, the concentrated PSS-coated GNR dispersions have an O.D. of 16.6 (586 μg/mL), and appear stable at room temperature or 4 °C for at least a year.

The peptizing qualities of PSS are dependent on initial loading levels and solution pH, as well the molecular weight and fine structure of the polyelectrolyte. In the case of 70-kDa PSS, the minimum concentration required to maintain a stable GNR dispersion at O.D. 1 was determined to be 33 μg/mL.[30] Furthermore, CTAB-coated GNRs have limited stability above pH 7,[22] so it is important to conduct the PSS coating procedure below this threshold pH. A convenient condition for peptization involves dispersing PSS and CTAB-coated GNRs in deionized water with previous exposure to atmospheric CO_2 (pH 5.2). The adsorption of PSS to the CTAB-coated GNRs increases their stability to environmental variations: they can maintain stable dispersions in phosphate buffered solution (PBS, pH 7.4, I=150 mM), and withstand basic solutions up to pH 12.5 (Figure 1A).

The molecular weight and amphiphilic character of the supporting polyelectrolyte are also important in GNR stabilization. GNRs treated with low molecular weight PSS (3.4 kDa) are much more prone to flocculation, presumably due to poor surface adsorption (Figure 1B). This is consistent with earlier studies of polymer adsorption which demonstrated the preferential accumulation of high molecular weight species onto solid surfaces.[31,32] We also evaluated a high molecular weight dextran sulfate (DSS, 100 kDa), another nontoxic polyelectrolyte which is superficially similar to PSS but considerably more hydrophilic. DSS was able to stabilize GNRs after multiple purification steps but was unable to support them in PBS solution, with an apparent dispersion half-life of just several hours. The large differences in peptization by PSS and DSS can be attributed to their ability to form complexes with residual CTAB on the GNR surface (see below).

NIH-PA Author Manuscript

NIH-PA Author Manuscript

NIH-PA Author Manuscript

Cytoxicity studies

GNRs were evaluated against three different cell lines, LLC-PK1 (porcine kidney), HepG2 (human liver carcinoma), and KB (human nasopharyngeal carcinoma), using standard viability tests based on MTT oxidation and LDH release (see Methods for details). A control study was conducted using CTAB-stabilized GNRs without PSS (CTAB-GNRs), which were introduced as serial dilutions from a stock solution containing CTAB slightly above CMC. CTAB-GNR dispersions were determined to have a cytotoxic effect at moderate loading levels; in the case of LLC-PK1 cells, a 24- or 48-h exposure to CTAB-GNRs yielded IC_{50} values of 12 and 8.3 μg/mL respectively, based on MTT assays (Table 1 and Figure 2A). Parallel studies with HepG2 and KB cells gave somewhat more complex results, but otherwise confirmed the toxicity of CTAB-GNRs. The amount of CTAB present in a 10 μg/mL GNR solution is estimated at 20 μM, which is within range of the IC_{50} values reported from previous cytotoxicity studies involving CTAB.[15-17]

LDH release provides complementary information to MTT assays, and the strong correlation in IC_{50} values suggests membrane disruption as the basis for acute cytotoxicity, implicating the active role of cationic amphiphiles (Table 1). We therefore consider the observed toxicity to be molecular in nature, and associated with the membrane-compromising effects of CTAB. This mode of action can also explain why the HepG2 cells are less affected than the KB and LLC-PK1 cells; HepG2 cells cultured under standard conditions typically express very few microvili on their outer membranes, which may decrease their surface area and sensitivity to solute adsorption relative to the other cell types.[33]

GNR dispersions treated with 70-kDa PSS and subjected to membrane ultrafiltration (PSS-GNRs) were evaluated and found to be even more toxic than CTAB-GNRs, contrary to expectations (Figure 2B). LLC-PK1 cells were again found to be the most sensitive, with MTT assays yielding IC_{50} values of 1.1 and 0.77 μg/mL after a 24- or 48-h exposure respectively; parallel studies with HepG2 and KB cells confirmed the heightened toxicity to be general (Table 1). The poor biocompatibility profile of the PSSGNRs was surprising given the minimal toxicity of both PSS and colloidal gold,[25] as well as the repeated attempts to remove CTAB by exhaustive dialysis.

To determine whether the cytotoxicity was directly associated with the GNRs, the PSS-GNR suspensions were resubjected to 100-kDa ultrafiltration, and separated into retentate and filtrate fractions. The separate evaluation of GNR retentate and filtrate revealed the source of cytotoxicity to lie with the latter, whereas the GNRs themselves were determined to be essentially nontoxic (Figure 3). Ultraviolet absorption spectroscopy of the filtrate indicated a significant amount of desorbed PSS (see below), leading us to suspect the source of cytotoxicity to be derived from a complex of PSS and residual CTAB. It is important to note that the cytotoxicity assays were performed 11 weeks after the PSS-GNRs were prepared and initially purified by ultrafiltration, strongly suggesting that much of the polyelectrolyte coating desorbed from the GNR surface during the interim.

The interactions between PSS and CTAB are well documented, and have been characterized by a variety of analytical methods.[34,35,36,37,38,39] These studies all indicate that the strong and essentially irreversible association of CTAB with PSS is due to complementary electrostatic and hydrophobic interactions. The free energy of binding of CTAB to PSS has been reported to be 32 kJ/mol, and is sufficient to prevent the passive resorption of CTAB into aqueous solution.[37] The PSS—CTAB complex is also more rigid than micellar CTAB, which may be a contributing factor in its activity. For example, a cryogenic TEM study of PSS polymer brushes on silica particles indicated the collapse of PSS chains into spikes when exposed to a CTAB concentration of 20 μM, well below the CMC value; the aggregates could not be undone by subsequent washing or exchange with inorganic cations.[39]

NIH-PA Author Manuscript

NIH-PA Author Manuscript

NIH-PA Author Manuscript

While the PSS—CTAB complex itself is very stable, its adsorption to the GNR surface is sufficiently weak that it can be removed by shear forces. Concentrated dispersions of PSS-GNRs contaminated with CTAB were centrifuged at 6,000 *g* for 5 minutes, then decanted and redispersed in a solution with unadulterated PSS (4–5 μg/mL/O.D.). The centrifugation—redispersion cycle could be repeated twice more to yield "CTAB-free" GNR suspensions stabilized by variable amounts of PSS (see below). To our satisfaction, these GNR dispersions exhibited greatly reduced toxicity towards KB cells, as ascertained by MTT assays following a 24-h incubation: The toxicity was reduced from an effective IC_{50} value of 3.7 μg/mL without PSS exchange to no appreciable toxicity at 85 μg/mL (highest concentration tested) after 3 times exchange with fresh PSS (Figure 4). This dramatic improvement in biocompatibility demonstrates that residual CTAB can be reduced to below cytotoxic levels by its removal as a PSS—CTAB complex.

The reversibility of polyelectrolyte adsorption implies that the amount of PSS introduced during the initial purification stages is not necessarily equal to the amount present in the final GNR dispersions. The level of PSS can be monitored after each processing step by absorption spectroscopy after appropriate dilution, based on a characteristic absorption peak at 225 nm which scales linearly with solute fraction between 0.7 and 20 μg/mL (Figure 5A). This provides a convenient means to estimate the weight ratio of PSS to GNR, by comparing peak absorptions at 225 nm (following subtraction of background absorption due to Au interband transitions) and at longitudinal plasmon resonance (LPR), respectively. For example, a GNR solution of O.D. 13.3 (470 μg/mL) treated with 70-kDa PSS at a loading of 33.3 μg/mL/O.D. has an approximate PSS/GNR weight ratio of 0.94. The PSS/GNR weight ratio decreases only slightly after several rounds of chloroform extraction and membrane dialysis, which upon dilution yields the absorption spectrum in Figure 5B. However, if the PSS-GNRs are centrifuged at speeds above 6000 *g* and the retentate is redispersed in deionized water, the PSS drops below optical detection limits (<0.02 O.D. or 0.175 μg/mL). The polyelectrolyte-depleted GNRs do not retain good dispersion stability in PBS, indicating that the shear forces experienced during centrifugation are sufficient to strip PSS (and coadsorbed CTAB) from the GNR surfaces.

Dispersion stability is temporarily restored by replenishing the GNR suspensions with fresh 70-kDa PSS, although not quite to the same levels observed prior to centrifugation and exhaustive CTAB removal. CTAB-free suspensions (O.D. 6) having a PSS/GNR weight ratio of 0.15 were observed to have a dispersion half-life in PBS on the order of 24 hours, with modest improvement at higher PSS/GNR ratios (Figure 6A). The tradeoff between biocompatibility and peptizing efficiency suggests that the initial adsorption of PSS to GNRs was assisted by its affinity for surface-bound CTAB, and thus weakened considerably by its removal. The loss of stabilization is congruent with the low peptizing activity of DSS (cf. Figure 1B), which does not have the capacity to form a stable complex with CTAB. More to the point, while CTAB-anchored PSS-GNRs can withstand passive membrane dialysis, they are not robust over longer periods of storage or against mechanical forms of surface desorption, and are thus less likely to survive the shear forces encountered during blood circulation *in vivo*. This set of observations, in conjunction with our *in vitro* cytotoxicity assays, confirms that PSS is poorly suited for maintaining GNR dispersion stability under physiological conditions.

The limited peptizing efficiency of PSS is not a serious concern, as it is easily replaced with other surface coatings. For example, GNRs cleansed by PSS treatment are readily stabilized by polyoxyethylene (20) sorbitan monolaurate (Tween 20), a nonionic surfactant known to stabilize colloidal Au nanoparticles[40] (Figure 6B). Other polyelectrolytes and nonionic surfactants can also be useful for mediating surfactant exchange; in particular, they can be replaced with chemisorptive surfactants, as recently illustrated for GNRs using a weakly basic polyelectrolyte resin.[41] With respect to GNR biocompatibility and dispersion stability in living

NIH-PA Author Manuscript

NIH-PA Author Manuscript

NIH-PA Author Manuscript

systems, methyl-terminated polyethyleneglycol (mPEG) chains can be grafted onto GNR surfaces by chemisorption, using either the standard alkylthiol approach[42,43] or by the *in situ* dithiocarbamate (DTC) method introduced by us.[19,44] mPEGDTC-coated GNRs have recently been shown to be inert to nonspecific cell uptake *in vitro*,[19] and therefore viable candidates for subsequent *in vivo* studies.

In summary, our studies indicate that PSS is useful as a mild detergent for detoxifying GNRs prepared under micellar CTAB conditions. The PSS conditioning protocol described here has been performed on a laboratory scale (30–50 mL), but the simplicity of the method is expected to be practical for process development and scaleup of "CTAB-free" GNRs. Ironically, PSS is less useful as a peptizing agent after the rigorous removal of CTAB from GNRs, but can be readily replaced by other types of nontoxic coatings, preferably ones which can survive mechanical shear forces and are inert to nonspecific cell uptake or adsorption of serum proteins.[19,42]

Methods

Synthesis of Au nanorods

All reagents were obtained from Sigma-Aldrich or Fluka and used as received unless otherwise stated. Deionized water was obtained using an ultrafiltration system (Milli-Q, Millipore) with a measured resistivity above 18 MΩ·cm, and passed through a 0.22-μm filter to remove particulate matter. GNRs were prepared with high-purity CTAB (SigmaUltra, >99%) using seeded growth conditions as previously described,[26,27] and treated with Na_2S to arrest further growth and changes in their optical resonances.[28] A GNR growth solution (400 mL) containing $HAuCl_4$ (0.5 mM), $AgNO_3$ (96 μM), ascorbic acid (0.54 mM) and CTAB (0.1 M) was treated with a cold solution of freshly prepared Au nanoparticle seeds (3–5 nm; 0.48 mL) and allowed to stand at room temperature for 50 min, then quenched by addition of a 4 mM Na_2S solution (100 mL) to yield a 500-mL suspension of GNRs with a longitudinal plasmon resonance (LPR) centered at 784 nm and an optical density (O.D.) of 0.8. The GNRs were separated and decanted from most of the supernatant by centrifugation at 24,000 *g* for 20 min, then resuspended in water to yield a highly concentrated sample of GNRs with a LPR centered at 786 nm (23 mL, O.D. *ca*. 16.8 based on 10× dilution).

Stabilization with polyelectrolytes

In a typical procedure, a suspension of highly concentrated, CTAB-stabilized GNRs (8 mL, O.D. 16.8) were combined with chloroform (8 mL) and agitated with a vortex mixer for 1 min to produce an emulsion. The phases were separated by centrifugation at 1,000 *g* for 4 min. The aqueous phase was removed and treated with a 1% w/v solution of PSS (70 kDa, 445 μL, then washed several more times with chloroform every 3 hours (3×8 mL). The polyelectrolyte-treated GNR suspension was further purified using a stirred ultrafiltration cell (Millipore, Model 8010) outfitted with a regenerated cellulose membrane having a nominal molecular weight limit (NMWL) of 100 kDa. The GNRs were subjected to 3 cycles of membrane ultrafiltration, with starting volumes of 200 mL and final volumes of 2 mL, 2 mL and 7.5 mL. The final dialyzed suspension of PSS-GNRs (O.D. *ca*. 16.6) could be serially diluted with PBS solution (pH 7.4); the diluted GNR dispersions exhibited a LPR peak at 785 nm and were stable at room temperature for at least 30 days. A similar procedure was performed for control experiments involving low-molecular weight PSS (3.4 kDa) and dextran sulfate sodium salt (DSS, 100 kDa).

"CTAB-free" GNRs were obtained by subjecting concentrated dispersions of PSS-GNRs to centrifugation at 6,000 *g* for 5 minutes to strip the CTAB-contaminated PSS coating from the GNR surface. The supernatant was decanted and the GNRs were redispersed in an aqueous

NIH-PA Author Manuscript

NIH-PA Author Manuscript

NIH-PA Author Manuscript

solution of unadulterated PSS (4–5 μg/mL/O.D.). The centrifugation—redispersion cycle was repeated twice more to yield PSS-coated GNR suspensions with minimal cytotoxicity.

Quantitative particle size analysis

Transmission electron microscopy (TEM) images were obtained using a Hitachi H7600 instrument operated at 80 kV. A 400-mesh Formvar carbon-coated copper grid was glow discharged in a vacuum evaporator (Denton) for 30 seconds to make the grid hydrophilic for favorable nanoparticle adsorption. The sample was prepared by dropping 3 μL of a GNR suspension onto the charged grid, then gently wicking the excess solution with filter paper after 30 seconds and allowing the residual wetting layer to dry in air. TEM analysis of PSS-coated GNRs indicated a mean length and midsection width of 71.5 ± 10.7 nm and 28.5 ± 7.3 nm, respectively (aspect ratio 2.6 ± 0.6). The GNRs were dumbbell-shaped and highly uniform, with fewer than 1% of the particles having an irregular structure (Figure 7A and B).

Aliquots of GNRs were also subjected to inductively coupled plasma optical emission spectroscopy (ICP—OES) in order to correlate O.D. with particle count. Comparison against a calibration standard yielded a gold content of 35.3 ppm (μg/mL) at O.D. 1, corresponding to a GNR concentration of 69 pM (4.15×10^{10} particles/mL) and an effective molar extinction coefficient of 1.45×10^{10} M^{-1} cm^{-1}. This value is higher than previously reported estimates,[45] mainly due to differences in particle volume. The concentration of the PSS-coated GNR stock solution (O.D. 16.6) is 586 μg/mL.

Dynamic light scattering (DLS) measurements were performed with Malvern Zetasizer Nano ZS and ZS90 instruments (Southborough, MA) with backscattering and 90° detectors, respectively. Hydrodynamic sizes are reported as intensity-weighted averages with a minimum of 12 measurements, and conducted in batch mode at 25 °C using low-volume polystyrene microcuvettes which were disposed after a single use. Stock samples were diluted 10- and 100-fold in phosphate buffered saline (PBS). Scattering intensities from these concentrations were collected with backscattering and 90° optics (Figure 8) and suggest an apparent bimodal size distribution, with the higher peak value corresponding to a hydrodynamic diameter (d_h) of 61.0 ± 0.8 nm for PSS-coated GNRs in PBS. The lower peak is not constant and shifted to a lower d_h value with the 90° collection optics, indicating that this peak is due to rotational and not translational diffusion. This information is thus omitted from the intensity-weighted average and polydispersity index of the final particle size distribution.

Zeta potential measurements

GNR samples were prepared at a concentration of 35 μg/mL in 10 mM NaCl. The pH of the sample was measured prior to loading into a pre-rinsed, folded capillary cell. Zeta potential measurements were performed using Malvern Zetasizer Nano ZS instrument at 25° C with an applied voltage of 150 V and a minimum of three measurements per sample. The zeta potential for PSS-stabilized GNRs at pH 8.8 is −51.2 ± 2.8 mV (Figure 9).

Cell culture conditions

All cell cultures were maintained in a 5% CO_2 environment at 37 °C. KB cells (derived from a human nasopharyngeal carcinoma) were grown to confluence in a folate-deficient cell culture medium (RPMI 1640, Gibco). The medium was supplemented with 10% fetal bovine serum (FBS, Sigma) and 1% penicillin—streptomycin (Invitrogen). Porcine renal proximal cells (LLC-PK1, ATCC) were maintained in Medium 199 with 3% FBS. Human hepatocarcinoma cells (Hep G2, ATCC) were maintained in RPMI 1640 with 2 mM L-glutamine and 10% FBS. Hep G2 cells were split 1 to 5, and limited to 20 passages.

NIH-PA Author Manuscript

NIH-PA Author Manuscript

NIH-PA Author Manuscript

Cell viability assay (MTT)

Cell survival was quantified by a colorimetric assay, based on the mitochondrial oxidation of 3-(4,5-dimethylthiazolyl-2)-2,5-diphenyltetrazolium bromide (MTT).[46,47] In a typical experiment, cells were harvested after passage and plated at a density of 2.5×10^5 cells/mL in 96-well microtiter format (100 μL/well), then incubated at 37 °C under a 5% CO_2 atmosphere and allowed to reach approximately 80% confluence. Cells were incubated for 6, 24, and 48 h with aliquots of PSS-coated GNR (20 μL) at varying concentrations, then treated with a freshly prepared 0.5% MTT solution (10 μL) and incubated for an additional 3 h before treatment with a 20% SDS solution in 1:1 DMF:H_2O (20 μL) adjusted to pH 4.7 to solubilize the formazan dye. Alternatively, the MTT media was removed, and the cells were fixed with DMSO (200 μL) plus 0.1 M glycine buffer (25 μL) adjusted to pH 10.5. The plates were left for 2 h in the dark, then assayed with an automated reader using an absorbance wavelength of 570 nm and a reference wavelength of 680 nm. The viability of GNR-treated cells was expressed as percent relative to cells treated with media alone. Aliquots of PSS-GNRs were prepared as serial dilutions from a stock solution in PBS with an initial concentration of 510 μg/mL; IC_{50} values were interpolated from the data points closest to 50% absorbance produced by positive control wells.

Lactose dehydrogenase (LDH) Release Assay—Membrane integrity, an indicator of cell viability, was quantified by a commercial colorimetric assay (Biovision #K311-400) based on the activity of LDH released from the cytoplasm of compromised cells. [48, 49] The LDH assay provides an estimate of membrane integrity by measuring the LDH-catalyzed oxidation of lactate to pyruvate, which reacts with the tetrazolium salt INT to form a formazan dye. Briefly, cells were harvested after passage and plated as previously described, and incubated for 6, 24, and 48 h with aliquots of PSS-coated GNR at varying concentrations. Aliquots of cell medium (100 μL) from each well were then mixed with 100 μL of the LDH assay solution, incubated in the dark for 20 min, then assayed with a plate reader at 490 nm.

Filtrate/Retentate Cytotoxicity Study—PSS-coated GNRs (aged for 11 weeks after preparation and purification, as described above) were separated from the suspension using a stirred ultrafiltration cell (Millipore, Model 8010) outfitted with a regenerated cellulose membrane having a nominal molecular weight limit (NMWL) of 100 kDa. The resulting GNR retentate was resuspended to its original volume in cell culture media, then diluted to 45 μg/mL. This was compared with an aliquot of the filtrate collected after ultrafiltration, diluted in similar fashion. LLC-PK1 cells were plated in 96-well microtiter format as previously described, and incubated for 48 h with the test materials. Cytotoxicity was determined using the MTT and LDH assays as described above.

Acknowledgments

The authors gratefully acknowledge financial support from the National Institutes of Health (EB-001777; NCI contract N01-CO-12400). The contents of this publication do not necessarily reflect the views or policies of the Department of Health and Human Services, nor does mention of trade names, commercial products, or organizations imply endorsement by the U.S. Government. Authors declare no competing financial interests. We thank Y. Zhao and Y. Wang (Harbin Institute of Technology) for helpful discussions, A. Oldenburg (Univ. of Illinois) for assistance with ICP-OES analysis, and T. Potter (NCL, SAIC-Frederick) for additional cytotoxicity assays.

References

1. Bentzen SM. Theragnostic Imaging for Radiation Oncology: Dose-Painting by Numbers. Lancet Oncol 2005;6:112–117. [PubMed: 15683820]
2. Cuenca AG, Jiang H, Hochwald SN, Delano M, Cance WG, Grobmyer SR. Emerging Implications of Nanotechnology on Cancer Diagnostics and Therapeutics. Cancer 2006;107:459–466. [PubMed: 16795065]

NIH-PA Author Manuscript

NIH-PA Author Manuscript

NIH-PA Author Manuscript

3. Ozdemir V, Williams-Jones B, Glatt SJ, Tsuang MT, Lohr JB, Reist C. Shifting Emphasis from Pharmacogenomics to Theragnostics. Nature Biotechnol 2006;24:942–946. [PubMed: 16900136]
4. Huff TB, Tong L, Zhao Y, Hansen MN, Cheng J-X, Wei A. Hyperthermic Effects of Gold Nanorods on Tumor Cells. Nanomedicine 2007;2:125–132. [PubMed: 17716198]
5. Tong L, Zhao Y, Huff TB, Hansen MN, Wei A, Cheng J-X. Gold Nanorods Mediate Tumor Cell Death by Compromising Membrane Integrity. Adv. Mater 2007;19:3136–3141.
6. Huang X, El-Sayed IH, Qian W, ElSayed MA. Cancer Cell Imaging and Photothermal Therapy in the Near-Infrared Region by Using Gold Nanorods. J. Am. Chem. Soc 2006;128:2115–2120. [PubMed: 16464114]
7. Black KC, Kirkpatrick ND, Troutman TS, Xu L, Vagner J, Gillies RJ, Barton JK, Utzinger U, Romanowski M. Gold Nanorods Targeted to Delta Opioid Receptor: Plasmon-Resonant Contrast and Photothermal Agents. Mol. Imaging 2008;7:50–57. [PubMed: 18384724]
8. Pissuwan D, Valenzuela SM, Killingsworth MC, Xu X, Cortie MB. Targeted Destruction of Murine Macrophage Cells with Bioconjugated Gold Nanorods. J. Nanoparticle Res 2007;9:1109–1124.
9. Pissuwan D, Valenzuela SM, Miller CM, Cortie MB. A Golden Bullet? Selective Targeting of Toxoplasma gondii Tachyzoites Using Antibody-Functionalized Gold Nanorods. Nano Lett 2007;7:3808–3812. [PubMed: 18034505]
10. Hirsch LR, Stafford RJ, Bankson JA, Sershen SR, Rivera B, Price RE, Hazle JD, Halas NJ, West JL. Nanoshell-Mediated Near-Infrared Thermal Therapy of Tumors Under Magnetic Resonance Guidance. Proc. Natl. Acad. Sci. USA 2003;100:13549–13554. [PubMed: 14597719]
11. Gobin AM, Lee MH, Halas NJ, James WD, Drezek RA, West JL. Near-Infrared Resonant Nanoshells for Combined Optical Imaging and Photothermal Cancer Therapy. Nano Lett 2007;7:1929–1934. [PubMed: 17550297]
12. Chen J, Wang D, Xi J, Au L, Siekkinen A, Warsen A, Li Z-Y, Hui Z, Xia Y, Li X. Immuno Gold Nanocages with Tailored Optical Properties for Targeted Photothermal Destruction of Cancer Cells. Nano Lett 2007;7:1318–1322. [PubMed: 17430005]
13. Zharov VP, Mercer KE, Galitovskaya EN, Smeltzer MS. Photothermal Nanotherapeutics and Nanodiagnostics for Selective Killing of Bacteria Targeted with Gold Nanoparticles. Biophys. J 2005;90:619–627. [PubMed: 16239330]
14. Zharov VP, Galitovskaya EN, Johnson C, Kelly T. Synergistic Enhancement of Selective Nanothermolysis with Gold Nanoclusters: Potential for Cancer Therapy. Lasers Surg. Med 2005;37:219–226. [PubMed: 16175635]
15. Cortesi R, Esposito E, Menegatti E, Gambari R, Nastruzzi C. Effect of Cationic Liposome Composition on in Vitro Cytotoxicity and Protective Effect on Carried DNA. Int. J. Pharm 1996;139:69–78.
16. Mirska D, Schirmer K, Funari S, Langner A, Dobner B, Brezesinski G. Biophysical and Biochemical Properties of a Binary Lipid Mixture for DNA Transfection. Colloids Surf. B 2005;40:51–59.
17. Takahashi H, Niidome Y, Niidome T, Kaneko K, Kawasaki H, Yamada H. Modification of Gold Nanorods Using Phosphatidylcholine to Reduce Cytotoxicity. Langmuir 2006;22:2–5. [PubMed: 16378388]
18. Connor EE, Mwamuka J, Gole A, Murphy CJ, Wyatt MD. Gold Nanoparticles Are Taken Up by Human Cells but Do Not Cause Acute Cytotoxicity. Small 2005;1:325–327. [PubMed: 17193451]
19. Huff TB, Hansen MN, Zhao Y, Cheng J-X, Wei A. Controlling the Cellular Uptake of Gold Nanorods. Langmuir 2007;23:1596–1599. [PubMed: 17279633]
20. Hayat, MA. Colloidal Gold: Principles, Methods, and Applications. Vol. 1. Academic Press; San Diego: 1989.
21. Gole A, Murphy CJ. Polyelectrolyte-Coated Gold Nanorods: Synthesis, Characterization and Immobilization. Chem. Mater 2005;17:1325–1330.
22. Ding H, Yong K-T, Roy I, Pudavar HE, Law WC, Bergey EJ, Prasad PN. Gold Nanorods Coated with Multilayer Polyelectrolyte as Contrast Agents for Multimodal Imaging. J. Phys. Chem. C 2007;111:12552–12557.
23. Kim K, Huang S-W, Ashkenazi S, O'Donnell M, Agarwal A, Kotov NA, Denny MF, Kaplan MJ. Photoacoustic Imaging of Early Inflammatory Response Using Gold Nanorods. Appl. Phys. Lett 2007;90:223901.

NIH-PA Author Manuscript

NIH-PA Author Manuscript

NIH-PA Author Manuscript

24. Durr NJ, Larson T, Smith DK, Korgel BA, Sokolov K, Ben-Yakar A. Two-Photon Luminescence Imaging of Cancer Cells Using Molecularly Targeted Gold Nanorods. Nano Lett 2007;7:941–945. [PubMed: 17335272]
25. Shepherd G, Klein-Schwartz W, Burstein AH. Efficacy of the Cation Exchange Resin, Sodium Polystyrene Sulfonate, to Decrease Iron Absorption. J. Toxicol. Clin. Toxicol 2000;38:389–394. [PubMed: 10930055]
26. Nikoobakht B, El-Sayed MA. Preparation and Growth Mechanism of Gold Nanorods (NRs) Using Seed-Mediated Growth Method. Chem. Mater 2003;15:1957–62.
27. Sau TK, Murphy C. J Seeded High Yield Synthesis of Short Au Nanorods in Aqueous Solution. Langmuir 2004;20:6414–6420. [PubMed: 15248731]
28. Zweifel DA, Wei A. Sulfide-Arrested Growth of Gold Nanorods. Chem. Mater 2005;17:4256–4261. [PubMed: 17415410]
29. Berr SS. Solvent Isotope Effects on Alkyltrimethylammonium Bromide Micelles as a Function of Alkyl Chain Length. J. Phys. Chem 1987;91:4760–4765.
30. Introducing PSS prior to the first chloroform wash is less efficient and requires a greater amount of polyelectrolyte, due to the significant formation of soluble PSS-CTAB complex.
31. Chibowski S. Dependence of the Adsorption Behavior of Poly(vinyl alcohol) at the Polystyrene Latex-Solution Interface on the Molecular Weight. J. Colloid Interf. Sci 1990;134:174–180.
32. Hlady V, Lyklema J, Fleer GJ. Effect of Polydispersity on the Adsorption of dextran on Silver Iodide. J. Colloid Interf. Sci 1982;87:395–406.
33. Ishigami A, Fujita T, Inoue H, Handa S, Kubo S, Kondo Y, Maruyama N. Senescence Marker Protein-30 (SMP30) Induces Formation of Microvilli and Bile Canaliculi in Hep G2 Cells. Cell Tissue Res 2005;320:243–249. [PubMed: 15714273]
34. Holmberg, K.; Jonsson, B.; Kronberg, B.; Lindman, B. Surfactants and Polymers in Aqueous Solution. John Wiley & Sons; Chichester, England: 2003.
35. Almgren M, Hansson P, Mukhtar E, van Stam J. Aggregation of Alkyltrimethylammonium Surfactants in Aqueous Poly(styrenesulfonate) Solutions. Langmuir 1992;8:2405–2412.
36. Maurdev G, Gee ML, Meagher L. Controlling the Adsorbed Conformation and Desorption of Polyelectrolyte with Added Surfactant via the Adsorption Mechanism: A Direct Force Measurements Study. Langmuir 2002;18:9401–9408.
37. Kogej K, Skerjanc J. Fluorescence and Conductivity Studies of Polyelectrolyte-Induced Aggregation of Alkyltrimethylammonium Bromides. Langmuir 1999;15:4251–4258.
38. Semchyschyn DJ, Carbone MA, Macdonald PM. Anionic Polyelectrolyte Binding to Mixed Cationic-Zwitterionic Surfactant Micelles: A Molecular Perspective from 2H NMR Spectroscopy. Langmuir 1996;12:253–260.
39. Samokhina L, Schrinner M, Ballauff M. Binding of Oppositely Charged Surfactants to Spherical Polyelectrolyte Brushes: A Study by Cryogenic Transmission Electron Microscopy. Langmuir 2007;23:3615–3619. [PubMed: 17316035]
40. Aslan K, Perez-Luna VH. Surface Modification of Colloidal Gold by Chemisorption of Alkanethiols in the Presence of a Nonionic Surfactant. Langmuir 2002;18:6059–6065.
41. Dai Q, Coutts J, Zou J, Huo Q. Surface Modification of Gold Nanorods through a Place Exchange Reaction Inside an Ionic Exchange Resin. Chem. Commun 2008:2858–2860.
42. Liao H, Hafner JH. Gold Nanorod Bioconjugates. Chem. Mater 2005;17:4636–4641.
43. Niidome T, Yamagata M, Okamoto Y, Akiyama Y, Takahashi H, Kawano T, Katayama Y, Niidome Y. PEG-Modified Gold Nanorods with a Stealth Character for *In Vivo* Applications. J. Control. Release 2006;35:500–501.
44. Zhao Y, PérezSegarra W, Shi Q, Wei A. Dithiocarbamate Assembly on Gold. J. Am. Chem. Soc 2005;127:7328–7329. [PubMed: 15898778]
45. Orendorff CJ, Murphy CJ. Quantitation of Metal Content in the Silver-Assisted Growth of Gold Nanorods. J. Phys. Chem. B 2006;110:3990–3994. [PubMed: 16509687]
46. Alley MC, Scudiero DA, Monks A, Hursey ML, Czerwinski MJ, Fine DL, Abbott BJ, Mayo JG, Shoemaker RH, Boyd MR. Feasibility of Drug Screening with Panels of Human Tumor Cell Lines Using a Microculture Tetrazolium Assay. Cancer Res 1988;48:589–601. [PubMed: 3335022]

NIH-PA Author Manuscript

NIH-PA Author Manuscript

NIH-PA Author Manuscript

47. Hansen MB, Nielsen SE, Berg K. Re-Examination and Further Development of a Precise and Rapid Dye Method for Measuring Cell Growth/Cell Kill. J Immunol. Methods 1989;119:203–210. [PubMed: 2470825]

48. Decker T, Lohmann-Matthes ML. A Quick and Simple Method for the Quantitation of Lactate Dehydrogenase Release in Measurements of Cellular Cytotoxicity and Tumor Necrosis Factor (TNF) Activity. J. Immumol Methods 1988;15:61–69.

49. Korzeniewski C, Callewaert DM. An Enzyme-Release Assay for Natural Cytotoxicity. J. Imuunol Methods 1983;64:313–320.

NIH-PA Author Manuscript

NIH-PA Author Manuscript

NIH-PA Author Manuscript

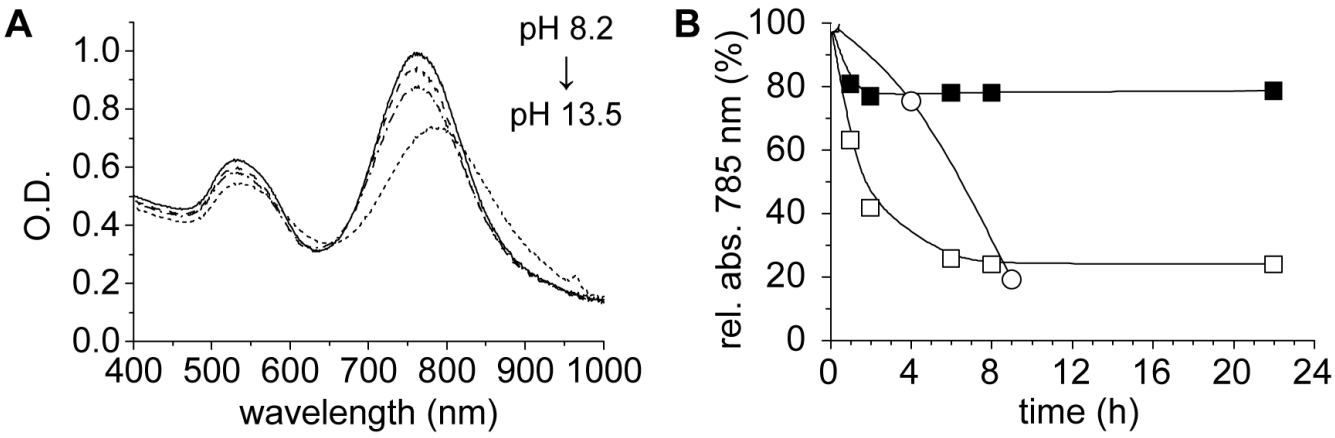

Figure 1.

(A) PSS-coated GNR dispersions over a range of pH values (8.2, 9.3, 11, 12.5, 13.5), after 24 h at room temperature. Samples were prepared by diluting concentrated GNR suspensions with buffer in a 10:1 ratio. (B) Stability of dialyzed GNRs dispersed in PBS solution (pH 7.4) over 24 h, using different peptizing agents: (■) 70-kDa PSS; (□) 3.4-kDa PSS; (○) 100-kDa DSS (weight ratio of peptizing agent to GNR=0.94). Lines drawn to guide the eye.

NIH-PA Author Manuscript

NIH-PA Author Manuscript

NIH-PA Author Manuscript

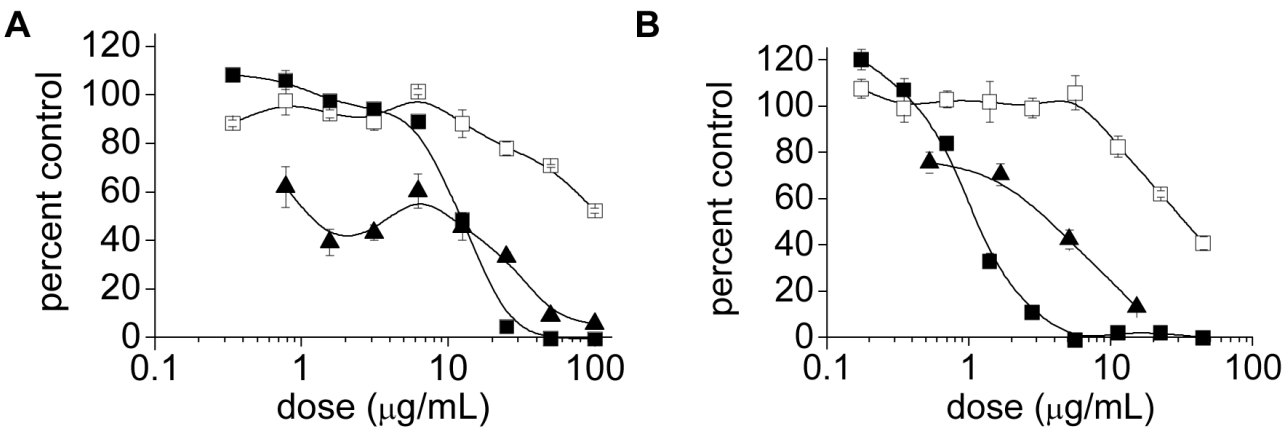

Figure 2.

Cytotoxicity of (A) CTAB-stabilized GNR dispersions and (B) GNR dispersions treated with 70-kDa PSS and subjected by ultrafiltration (aged for 11 weeks), based on a MTT viability assay after a 24-h exposure (pH 7.4): (■) LLC-PK1 cells; (□) HepG2 cells; (▲) KB cells. All MTT viability data are normalized with respect to a media-only control. Lines drawn to guide the eye.

NIH-PA Author Manuscript

NIH-PA Author Manuscript

NIH-PA Author Manuscript

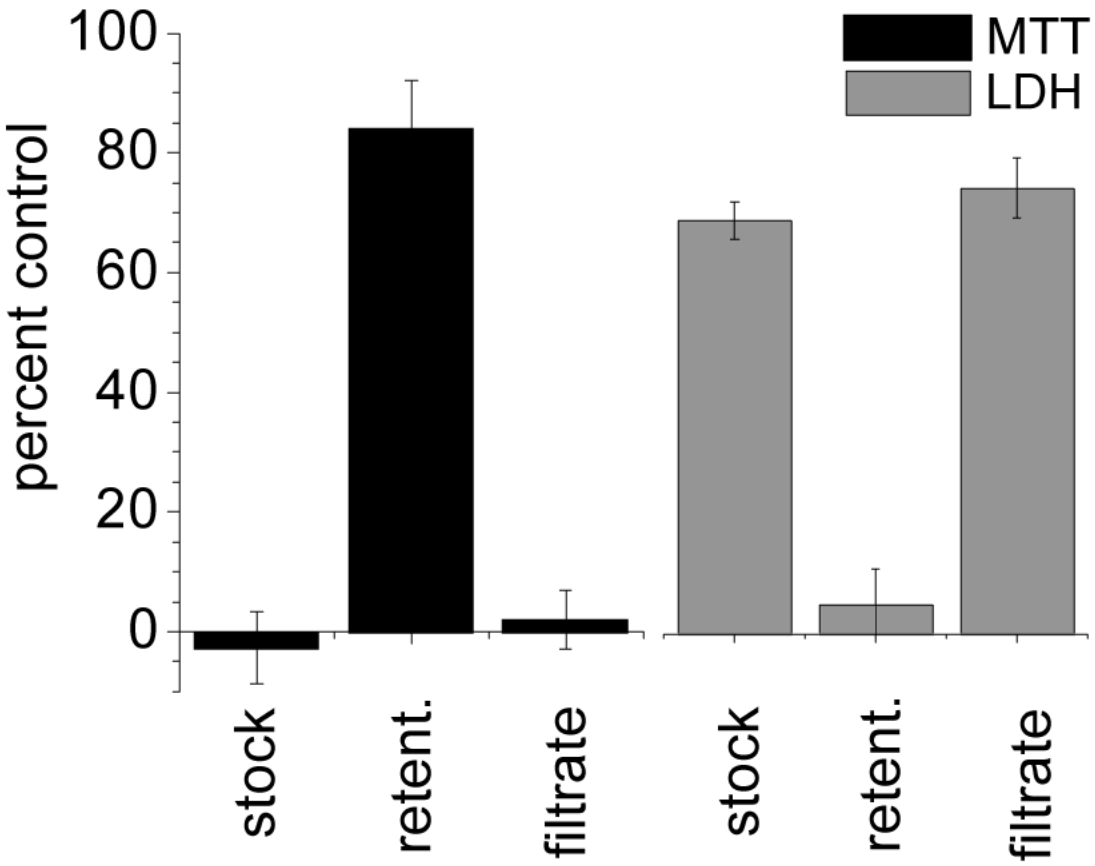

Figure 3.
MTT and LDH assays establishing the viability and membrane integrity, respectively, of LLC-PK1 cells after incubation over 48 h with the following: 45 μg/mL GNR stock solution; 100-kDa retentate (after resuspension in fresh media); 100-kDa filtrate. Percentage values are normalized with respect to a media-only control.

NIH-PA Author Manuscript

NIH-PA Author Manuscript

NIH-PA Author Manuscript

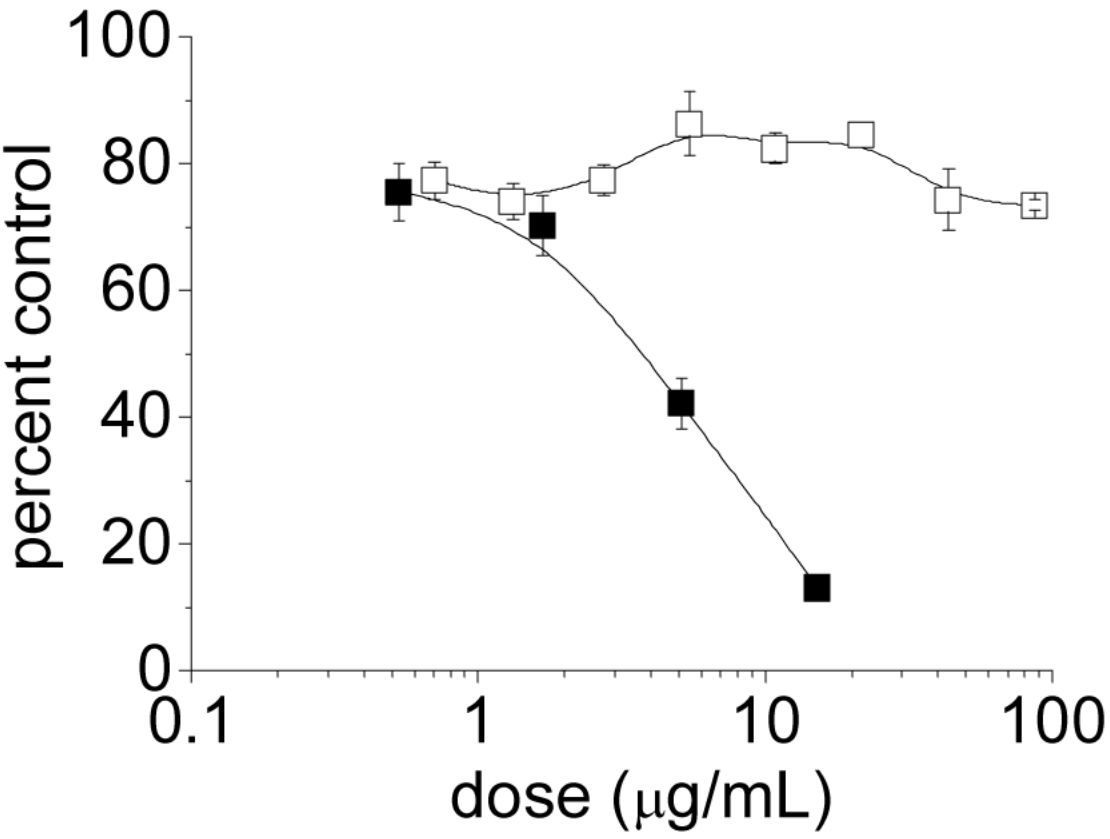

Figure 4.
MTT cytotoxicity profile of PSS-coated GNRs using KB cells, before and after exchange with unadulterated PSS. (■) PSS-coated GNRs contaminated with CTAB (prior to PSS exchange); (□) "CTAB-free" GNRs after three times exchange and redispersion with 70-kDa PSS (4.4 μg/mL/O.D.; PSS/GNR weight ratio of 0.12). Lines drawn to guide the eye.

NIH-PA Author Manuscript

NIH-PA Author Manuscript

NIH-PA Author Manuscript

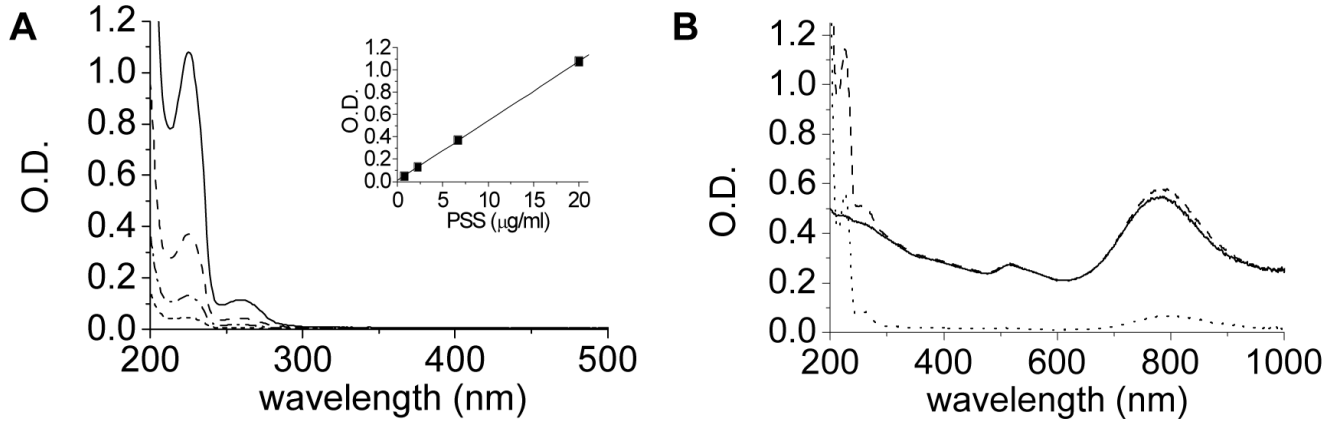

Figure 5.

Absorption spectroscopy of PSS and PSS-GNRs. (A) Linear absorption range of PSS (free polyelectrolyte; slope=0.053). (B) PSS-GNRs purified by membrane ultrafiltration (---); GNRs after centrifugation (6000 *g*, 5 min) and redispersion in deionized water (—); supernatant containing PSS stripped from GNRs (???).

NIH-PA Author Manuscript

NIH-PA Author Manuscript

NIH-PA Author Manuscript

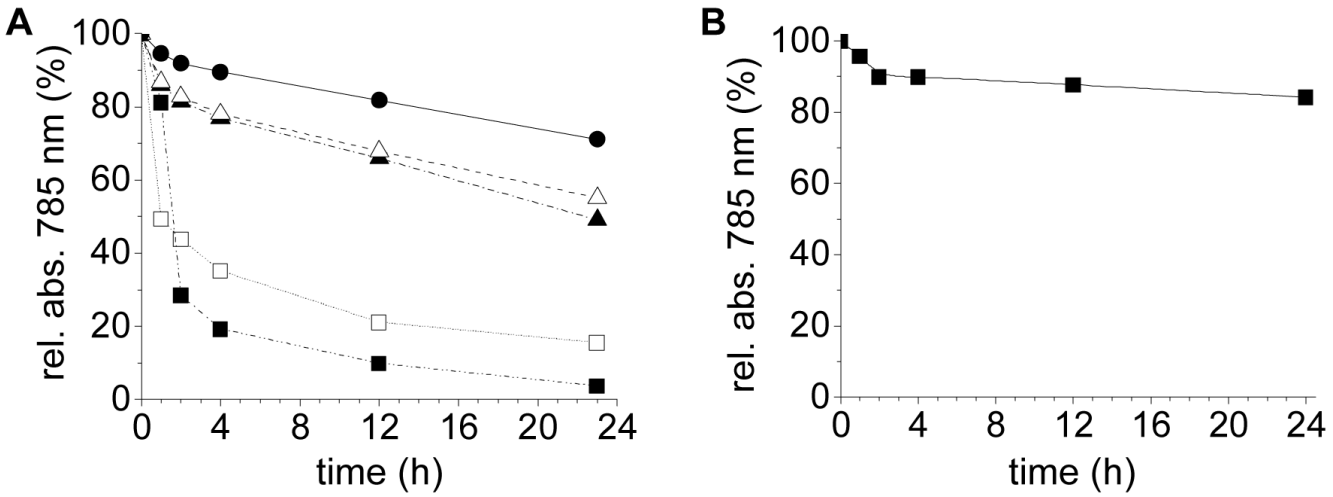

Figure 6.

(A) Dispersion stability of GNRs in PBS (pH 7.4), following centrifugation (6000 *g*) and 3× exchange with 70-kDa PSS at 4.4 μg/mL/O.D. (PSS/GNR = 0.12), then dispersed at different PSS/GNR weight ratios: (□) no PSS added; (■) PSS/GNR = 0.06; (▲) PSS/GNR = 0.15; (△) PSS/GNR = 0.37; (•) PSS/GNR = 0.98. (B) GNR dispersion stability in PBS following 3× exchange with 70-kDa PSS (4.4 μg/mL/O.D.) and redispersion in Tween 20 at a final concentration of 4 mM (*ca*. 5 μg/mL). Lines drawn to guide the eye.

NIH-PA Author Manuscript
NIH-PA Author Manuscript
NIH-PA Author Manuscript

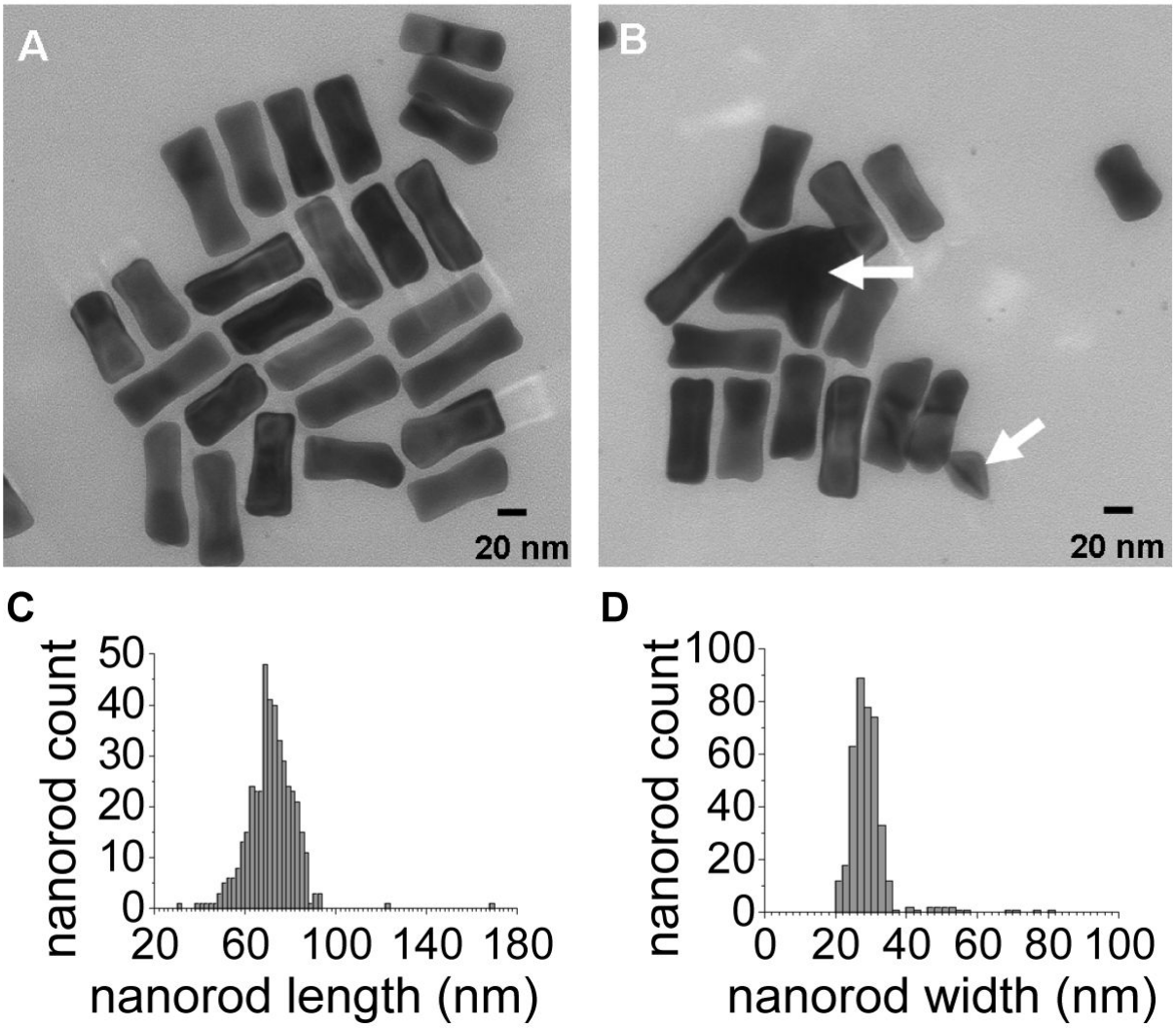

Figure 7.

(A, B) Representative TEM images of PSS-stabilized GNRs; (C, D) histogram of GNR length and width distribution (71.5 ± 10.7 nm and 28.5 ± 7.3 nm, respectively; *N*=426). Less than 1% of the observed particles were irregularly shaped (marked with white arrows in B).

NIH-PA Author Manuscript

NIH-PA Author Manuscript

NIH-PA Author Manuscript

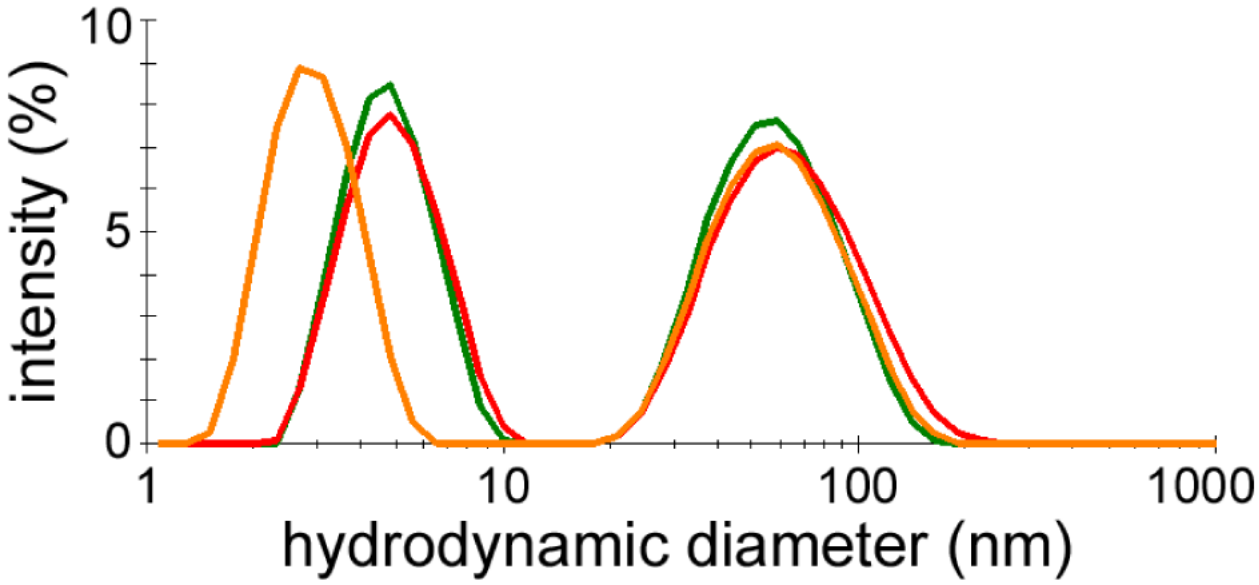

Figure 8.
Intensity-averaged size distribution plots of PSS-stabilized GNRs in PBS, at 35 μg/mL with backscattering optics (green trace) and 90° collection optics (orange trace), and at 3.5 μg/mL with backscattering optics (red trace). Peaks below 10 nm are due to rotational diffusion and have been omitted from size distribution analysis. Traces are based on a minimum of 12 measurements per sample.

NIH-PA Author Manuscript

NIH-PA Author Manuscript

NIH-PA Author Manuscript

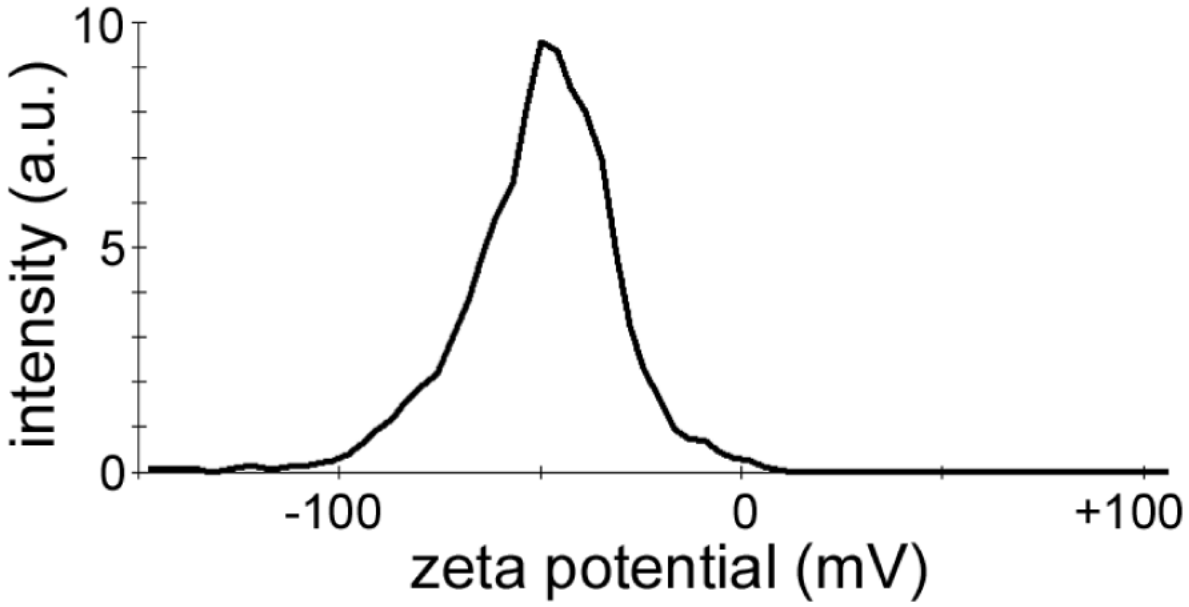

Figure 9.
Zeta potential distribution of PSS-stabilized GNRs at pH 8.8, in 100 mM NaCl. The trace in the figure is based on the average of three measurements.

NIH-PA Author Manuscript NIH-PA Author Manuscript NIH-PA Author Manuscript

Table 1

IC_{50} values (μg/mL) of CTAB-stabilized GNRs, before and after treatment with 70-kDa PSS [a]

	CTAB-GNRs				PSS-GNRs[b]			
	LLC-PK1		HepG2		LLC-PK1		HepG2	
t **(h)**	**MTT**	**LDH**	**MTT**	**LDH**	**MTT**	**LDH**	**MTT**	**LDH**
24	12	11	>100	>100	1.1	1.0	33	45
48	8.3	5.5	78	>100	0.77	0.56	22	22

[a] All experiments run in triplicate.

[b] GNRs were subject to stirred-cell ultrafiltration (100 kDa MWCO) prior to testing to remove excess CTAB and PSS.